Biophysical Characterization of the Type III Secretion System Translocator Proteins and the Translocator Proteins Attached to Bacterium-Like Particles

XIAOTONG CHEN,[1] SHYAMAL P. CHOUDHARI,[1] PRASHANT KUMAR,[1] RONALD T. TOTH IV,[2] JAE HYUN KIM,[2] MAARTEN L. VAN ROOSMALEN,[3] KEES LEENHOUTS,[3] C. RUSSELL MIDDAUGH,[1,2] WENDY L. PICKING,[1] WILLIAM D. PICKING[1]

[1]Department of Pharmaceutical Chemistry, University of Kansas, Lawrence, Kansas
[2]Macromolecule and Vaccine Stabilization Center, University of Kansas, Lawrence, Kansas
[3]Mucosis BV, Groningen, The Netherlands

Received 12 March 2015; revised 12 August 2015; accepted 2 September 2015

Published online 30 September 2015 in Wiley Online Library (wileyonlinelibrary.com). DOI 10.1002/jps.24659

ABSTRACT: Diarrhea caused by *Shigella, Salmonella,* and *Yersinia* is an important public health problem, but development of safe and effective vaccines against such diseases is challenging. A new antigen delivery platform called bacterium-like particles (BLPs) was explored as a means for delivering protective antigens from the type III secretion systems (T3SS) of these pathogens. BLPs are peptidoglycan skeletons derived from *Lactococcus lactis* that are safe for newborns and can carry multiple antigens. Hydrophobic T3SS translocator proteins were fused to a peptidoglycan anchor (PA) for BLP attachment. The proteins and protein–BLP complexes associated with BLPs were characterized and the resulting data used to create three-index empirical phase diagrams (EPDs). On the basis of these EPDs, IpaB (S*higella*) and SipB (*Salmonella*) behave distinctly from YopB (*Yersinia*) under different environmental stresses. Adding the PA domain appears to enhance the stability of both the PA and translocator proteins, which was confirmed using differential scanning calorimetry, and although the particles dominated the spectroscopic signals in the protein-loaded BLPs, structural changes in the proteins were still detected. The protein–BLPs were most stable near neutral pH, but these proteins' hydrophobicity made them sensitive to environmental stresses. © 2015 Wiley Periodicals, Inc. and the American Pharmacists Association J Pharm Sci 104:4065–4073, 2015
Keywords: circular dichroism; fluorescence spectroscopy; light scattering (static); pH; physical stability

INTRODUCTION

Diarrheal infections are an important public health problem and a major cause of morbidity globally, particularly in developing countries. Among the many pathogens causing infectious diarrhea, *Shigella*, *Salmonella*, and *Yersinia enterocolitica* are important because of their high morbidity rates, ease of transmission, increasing incidence of antibiotic resistance, and the current lack of effective vaccines.[1] Infants and young children under 5 years are the most vulnerable to diarrheal disease because they can quickly succumb to severe dehydration. Furthermore, repeated diarrheal episodes exacerbate malnutrition and can cause stunted growth and impaired cognitive development.[2]

Like many other Gram-negative bacteria, *Shigella* spp, *Salmonella enterica*, and *Yersinia* spp. all possess the type III secretion system (T3SS) as a common virulence factor. The T3SS has a syringe-like structure that forms an energized conduit for the injection of effector proteins into host cells via a surface-localized needle. Located at the needle tip is a "tip complex" that is responsible for protein secretion control and consists of a tip protein and translocator proteins.[3,4] In the presence of certain small molecule triggers, the first translocator is proposed to become localized externally to the tip protein where it then initiates contact with a host cell. These translocator proteins are IpaB, SipB, and YopB for *Shigella*, *Salmonella*, and *Yersinia*, respectively. Because of their surface exposure and essential roles in virulence, these T3SS proteins are attractive targets for inclusion in a protective vaccine. More importantly, as these proteins are very highly conserved at the sequence level within a given genus, they have the potential to be broad spectrum vaccine candidates capable of providing serotype-independent protection.

Even without direct contact with contaminated water, children can be infected by *Shigella, Salmonella*, and *Yersinia enterocolitica* through contact with ill individuals via the fecal-oral route. Thus, development of vaccines against these pathogens is a critical need. Vaccination is one of the most effective public health tools for the prevention of infectious diseases. Formulation of safe and effective vaccines for newborns and infants against infectious disease, however, can be challenging. Subunit vaccines are usually safe to administer but typically require a suitable adjuvant and delivery system to increase efficacy. A novel technology using modified *Lactococcus lactis* cell wall particles as a platform for antigen delivery (referred to as bacterium-like particles or BLPs) has recently been developed.[5,6] *L. lactis* is a Gram-positive, nonpathogenic lactic acid bacterium that is widely used in the production of dairy-based food products and is considered a generally regarded as safe entity.[7] *L. lactis* is one of the probiotics that has been shown to be safe for children and even newborns.[8] BLPs are produced from fresh *L. lactis* employing harsh acidic treatment to remove the DNA, RNA, lipids, and almost all of the associated bacterial proteins, but the peptidoglycan envelope remains

Correspondence to: William D. Picking (Telephone: +785-864-5974; Fax: +785-864-1916; E-mail: picking@ku.edu)
This article contains supplementary material available from the authors upon request or via the Internet at http://wileylibrary.com.

Journal of Pharmaceutical Sciences, Vol. 104, 4065–4073 (2015)

intact. The entire BLP production process is simple and relatively inexpensive, and the final product is stable at room temperature. BLPs can be administered at mucosal sites, which is more "friendly" to infants than needle injection. In addition to these desirable features, BLPs possess immune-stimulation properties conveyed by the peptidoglycan nature of their structure that activates the innate immune system through TLR2-mediated signaling.[9,10]

As a delivery system, a BLP provides a scaffold for carrying multiple subunit antigens on its surface. To attach antigens to the BLP surface, the antigens can be produced as fusions proteins containing a peptidoglycan anchor (PA) domain that is also derived from *L. lactis*. The recombinant antigen-P-A fusion proteins are noncovalently bound to BLPs, but the association is extremely tight.[11] Because of the nature of the platform, a single or multiple antigens can be displayed on a single BLP's surface or BLPs carrying different antigens can be mixed, allowing the presentation of a wide variety of protein antigens from different pathogens. The self-adjuvanting platform provided by BLPs has been employed for vaccine development against different pathogens including pneumococcus, malaria, RSV, and influenza virus.[5,12–14]

For protein-based vaccines, a major concern regarding formulation is stability in aqueous solution during storage and transport. Temperature and pH are critical factors that influence protein stability. Naked BLPs are highly stable at room temperature, but for BLPs with associated proteins, formulation conditions are less established. Therefore, a variety of biophysical techniques are used here to characterize the stability of the protein-containing complex as a function of pH and temperature. The main techniques used here to monitor protein structural state are circular dichroism (CD), intrinsic fluorescence, and static light scattering (SLS) spectroscopies. These multiple methods give rise to large amounts of data, so the findings generated here are summarized in three-index empirical phase diagrams (EPDs). Furthermore, to better understand the effect of binding of PA fusion proteins to BLPs, we compared the biophysical studies of T3SS proteins alone, fused with the PA domain, and the fusion after attachment to BLPs. For T3SS needle tip proteins, the PA domain was added at the C-terminus, but this strategy led to poor expression and stability for the translocator proteins (unpublished results). As a result, the translocator proteins were designed with the PA domain attached at their N-termini. Furthermore, IpaB, SipB, and YopB are hydrophobic proteins and need to be coexpressed with their specific chaperones (IpgC, SicA, and SycD, respectively). This also applies to expression of PA–IpaB, PA–SipB, and PA–YopB. After initial purification, the chaperones were removed using the detergent lauryldimethylamine N-oxide (LDAO), which is also needed to maintain the solubility of the resulting individual translocator proteins. Thus, for the characterization of the translocator proteins, the PA fusions and PA fusions associated with BLPs, LDAO was present at all times.

MATERIAL AND METHODS

Generation of Plasmids for Expression of the First Translocator Protein Genes in *E. Coli*

The *ipaB*, *sipB*, and *yopB* genes were amplified by PCR using a 5′ primer with *Nde*I restriction site and a 3′ primer with *Bam*HI restriction site. The PCR products were digested and ligated into pET15b. The constructed pET15b plasmids were used to transform *E. coli* NovaBlue. The translocator protein chaperone genes *ipgC*, *sicA*, and *sycD* were amplified by PCR and ligated into pACYCDuet-1 that was used to cotransform *E. coli* Tuner (DE3) for coexpression. Bacteria containing both plasmids were selected using ampicillin and chloramphenicol.

Generation of Plasmids for Expression of PA–First Translocator Protein Genes in *E. Coli*

The *ipaB*, *sipB*, and *yopB* genes were amplified by PCR using a 5′ primer with an *Nde*I restriction site and a 3′ primer with a *Bam*HI restriction site, whereas the *pa* (encoding the *L. lactis* PA peptide) was generated using both 5′ primer and 3′ primers with *Nde*I sites. The PCR product was digested and ligated into pET15b to form the *pa–ipaB*, *pa–sipB*, and *pa–yopB* constructs. The resulting pET15b was used to transform *E. coli* NovaBlue cells. The cognate translocator protein chaperone genes *ipgC*, *sicA*, and *sycD* were cloned into pACYCDuet-1. *pa–ipaB*/pET15b+*ipgC*/pACYC-1 or *pa–sipB*/pET15b+*sicA*/pACYC-Duet-1 were used to cotransform *E. coli* tuner (DE3) for coexpression, whereas the *pa–yopB*/pET15b+*sycD*/pACYC-Duet-1 that is transformed into the *E. coli* C43 strain. Both plasmids were selected using ampicillin and chloramphenicol.

Expression and Purification of the Translocator Proteins

IpaB and IpgC (IpaB/IpgC) were coexpressed using autoinduction media, whereas SipB/SicA and YopB/SycD were coexpressed using Terrific broth media. The proteins were purified using standard IMAC purification conditions. IpaB/IpgC was further purified using hydrophobic interaction chromatography, whereas SipB/SicA was further purified using anion exchange chromatography. A second IMAC step was used for all three proteins to remove chaperones using buffers containing LDAO. The final products were dialyzed into phosphate-buffered saline (PBS) containing 0.05% (w/v) LDAO.

Expression and Purification of the PA–Translocator Proteins and Production of Translocator Protein–BLPs

All three translocator proteins possessing a PA tag at their N-termini were expressed using Terrific broth media. Harvested cells were lysed and the proteins were purified using standard IMAC procedures from the clarified supernatant. PA–IpaB/IpgC and PA–SipB/SicA were further purified using anion exchange chromatography followed by a second IMAC with LDAO present to remove the chaperone. The final products were dialyzed into PBS containing 0.05% (w/v) LDAO. PA–YopB/SycD was further purified using size-exclusion chromatography with PBS containing LDAO. The final translocator protein products were incubated with naked BLPs at room temperature for 2 h and washed thoroughly with PBS 0.05% (w/v) LDAO.

Biophysical Characterization of the Protein Preparation

The translocator proteins and PA–translocator proteins used in biophysical analyses were dialyzed into 20 mM citrate phosphate (CP) buffer containing LDAO at each pH from pH 3.0 to 8.0. The ionic strength of the buffer was adjusted to 0.15 using NaCl. The dialyzed proteins were then filtered through 0.22-μm Millex Syringe-driven filters. The concentration of the proteins

was calculated based on UV_{280} absorbance and the individual extinction coefficients (Supplemental Table 1). The concentrations of PA–translocator proteins were adjusted to 0.15 mg/mL and translocator proteins were adjusted to 0.3 mg/mL.

The protein–BLPs were centrifuged and resuspended in CP buffer containing LDAO at one unit pH intervals from 3 to 8. The ionic strength of the buffer was adjusted to 0.15 with NaCl. The centrifugation–resupsension process was repeated three times to thoroughly wash the protein–BLPs and equilibrate the pH. All the protein–BLPs samples were diluted to contain 1 mg BLP/mL. This corresponded to 0.12 mg/mL for PA–IpaB, 0.11 mg/mL of PA–SipB, and 0.07 mg/mL of PA–YopB, because of protein-specific binding capacities.

Far-UV CD Spectroscopy

Circular dichroism spectra of all protein samples at each pH (3.0–8.0) were measured using a Jasco J-815 CD spectrometer equipped with a six-position Peltier temperature controller. The spectra were collected from 260 to 190 nm at 10°C at a scanning speed of 50 nm/min, 1.0 nm resolution, and three data acquisitions. Thermal unfolding was measured by collecting the CD signal at 222 nm (225 nm for proteins bound to BLPs) every 2.5°C from 10°C to 90°C, employing a temperature ramp rate of 15°C/h. Samples were equilibrated to the target temperature (°0.1°C) for 5 s prior to each data point measurement. Each sample was measured in triplicate and buffer blanks were subtracted prior to data analysis. The data for the proteins were converted to molar ellipticity using Jasco Spectra Manager (Jasco Inc., Easton, MD) and Origin 8.6 software (Origin Labs Corp., Northhampton, MA).

Intrinsic Tryptophan Fluorescence Spectroscopy

Intrinsic tryptophan (Trp) fluorescence spectra of all the samples were obtained using a Photon Technology International (PTI) spectrofluorometer (Birmingham, New Jersey) equipped with a turreted 4-position Peltier-controlled cell holder (Quantum Northwest, Washington). Trp residues were excited selectively at 295 nm, and the emission spectra were acquired from 300 to 400 nm employing a step size of 1 nm and a 0.5-s integration time. The emission spectra were collected in 1-cm pathlength cuvettes every 2.5°C as a function of temperature from 10°C to 85°C using a 3-min equilibration time. The samples were measured in triplicates and spectra of blank buffers at each pH were subtracted from the sample spectra. Peak positions were obtained using a mean spectral center of mass (msm) method using Origin 8.6 software (Origin Labs). The emission peak position calculated by the msm method are shifted higher by 10–14 nm from actual peak positions; however, the data obtained by this method display improved signal to noise ratio.

Static Light Scattering

Static light scattering provides a measure of thermally induced protein aggregation. These measurements were acquired simultaneously with intrinsic Trp fluorescence measurements using a second detector oriented 180° from the fluorescence photomultiplier tube but still 90° relative to the excitation source. Light scattering intensity at 295 nm was monitored as a function of temperature every 2.5°C over a temperature range of 10°C–85°C. Buffer scans were subtracted from the sample readings prior to data analysis.

Three-Index EPDs

The multivariant thermal stability data acquired from the multiple techniques for each protein sample were summarized for global analysis using a three-index EPD to provide a comprehensive overview of the data using a standardized red, green, and blue (RGB) color scheme.[15] Briefly, the degree of structural changes as a function of different environmental stress conditions is calculated for each data set. In this study, the secondary structural index was calculated from the 222-nm CD molar ellipticity (225 nm for proteins associated with BLPs), the tertiary structural index was calculated from intrinsic Trp fluorescence peak position, and the quaternary structure index (aggregation) was calculated from the SLS data. The values for the structural indices were normalized from 0 to 1. For secondary and tertiary structure, 1 represents native structure, whereas 0 represents extensively altered structure. However, for the aggregation index, 0 indicates no aggregation, whereas 1 indicates the maximum extent of aggregation. Each of the structural indices was assigned to a color in a standardized RGB color scheme. Secondary structure was assigned to red color, whereas tertiary structure was assigned to green. Aggregation was assigned to blue color and minimal or no aggregation was assigned to black. The EPDs represented physical states of the protein at each pH-temperature condition examined using a combination of the color scheme, whereas each RGB component can be seen in the right hand panels next to the associated EPD.

Differential Scanning Calorimetry

Differential scanning calorimetry (DSC) was performed using an Auto-VP capillary differential scanning calorimeter (MicroCal/Malvern Instruments, Worcestershire, United Kingdom) equipped with Tantalum sample and reference cells. The cells were pressurized with dry nitrogen at approximately 65 psi. Two water–water scans were taken prior to the reference and sample scans. Scans were completed from 10°C to 100°C using a scan rate of 60°C/h and a concentration of 2 mg/mL. The syringe, injector, and cells were cleaned prior to each scan. Reference subtraction and concentration normalization were performed using the instrument software.

RESULTS

Biophysical Characterization of IpaB, SipB, and YopB

The translocator proteins IpaB, SipB, and YopB were coexpressed with their chaperones that were removed with the detergent LDAO.[16] The biophysical characterization of these proteins was conducted in the presence of LDAO to maintain each protein's solubility. For IpaB and SipB, minor chemical degradation was seen using SDS-PAGE analysis at pH 3, and this was even more pronounced for PA–IpaB and PA–SipB. To reduce the complexity and focus on the effect the PA domain brings to these proteins, pH 3 was eliminated from the study for these proteins. In contrast, no degradation was seen for YopB, so it was studied at pH 3–8. Far-UV CD spectroscopy for the translocator proteins revealed double minima at 208 and 222 nm under each pH condition, indicating dominant α-helical content (Supplemental Figs. S1A, S2A, and S3A). Thus, as seen previously for a fusion protein consisting of *Shigella* IpaD (tip protein) and IpaB (called DB fusion or DBF),[16] the presence

of LDAO seemed to have a stabilizing effect at low pH for the translocator proteins.

The thermal stability of each protein's secondary structure was determined by monitoring the CD signal (molar ellipticity at 222 nm) as a function of temperature (Supplemental Figs. S1B, S2B, and S3B). The secondary structure signal of IpaB at pH 4–6 indicated a gradual transition in the CD data as the temperature was increased, whereas a sharper transition at pH 7 and 8 was observed between 45°C and 50°C. A partially unfolded state was reached at all pH values after reaching 90°C. Interestingly, when the protein was cooled after the thermal melt, it exhibited a CD spectrum identical to the one observed before the melt (data not shown). This indicates that in the presence of LDAO, IpaB recovers its secondary structure when cooled. A similar pattern was seen for SipB, although there were less obvious transitions. On the contrary, the amount of secondary structure of YopB appeared to be less at each pH tested based on the lower initial CD signal at 10°C. Nevertheless, clear thermal transitions in the YopB secondary structure were observed at approximately 60°C–70°C at pH 5, 6, and 7. In contrast, gradual changes in secondary structure content were observed as the temperature was raised at pH 3, 4, and 8.

Changes in the tertiary structure of the proteins were monitored using intrinsic fluorescence peak position as a function of pH and temperature (Supplemental Figs. S1C, S2C, and S3C). For IpaB, the initial peak position at 10°C at pH 4 and 5 was observed to be slightly higher (by 1 nm) than at pH 7 and 8, indicating possible minor structural perturbation of IpaB under low pH conditions. The opposite pattern, however, was seen for SipB and YopB. In agreement with the CD data, IpaB displayed a pronounced red shift in the Trp peak position at all pH values as the temperature was increased with transitions occurring at approximately 50°C, suggesting loss of tertiary structure (Fig. S1C). Meanwhile, an increase in peak position was observed for SipB, suggesting a gradual and probably small change in tertiary structure occurs in response to the thermal stress. For YopB, transition trends similar to those seen at elevated temperatures in the CD unfolding curves were observed, although no sharp transitions were seen.

Static light scattering was performed simultaneously with the intrinsic fluorescence measurements to determine the aggregation state of IpaB, SipB, and YopB as a function of pH and temperature (Supplemental Figs. S1D, S2D, and S3D). LDAO has been shown to prevent aggregation of the DB fusion.[16] IpaB and SipB were also found to largely resist thermally induced aggregation in the presence of LDAO. No significant increase in light scattering was observed for SipB regardless of temperature and pH, indicating no aggregation occurred. Notably, IpaB showed a slight increase in the light scattering intensity as the thermal stress was increased at pH 7 and 8. Although the signal changes were relatively small, the transition temperatures appeared to match those seen using the other techniques. At no time were visible aggregates observed. In contrast to IpaB and SipB, a relatively higher light scattering signal was observed at 10°C for YopB. An onset of aggregation was then observed at approximately 60°C at pH 5 for YopB that resulted in a further increase in the scattering intensity. The SLS data also revealed a rapid decrease in the scattering intensity for YopB at approximately 60°C and above at pH 6 and 7, probably as a result of aggregation/precipitation, which is consistent with destabilization of YopB. Interestingly, no abrupt change in the SLS intensity was observed at pH 3, 4, and 8, and the

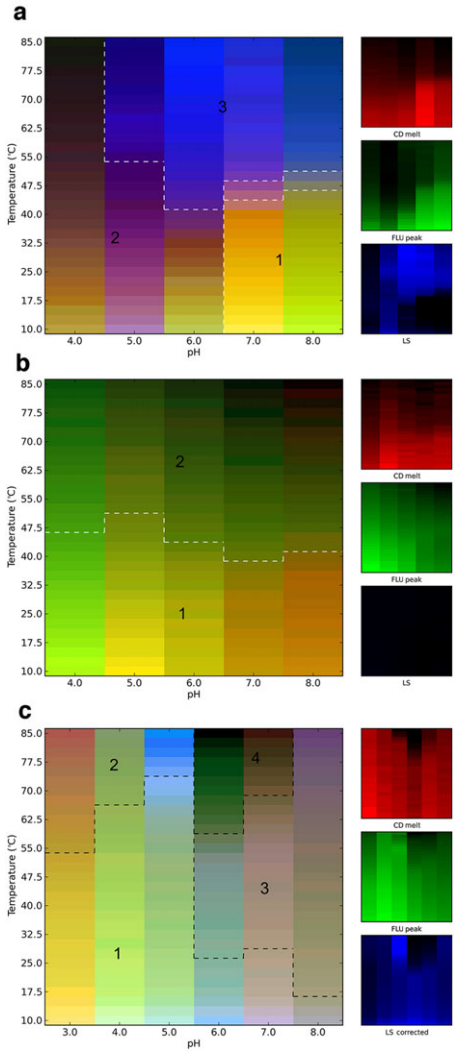

Figure 1. Three-index EPDs with LDAO present for IpaB (a), SipB (b), and YopB (c), representing the conformational stability of the translocator proteins as a function of pH and temperature. The red, green, and blue panels at the right define individual component indices for secondary structure (CD), tertiary structure (fluorescence peak position), and aggregation behavior (LS), respectively.

light scattering intensity decreased initially in all cases as the temperature was raised from 10°C to 20°C. It is possible that this is because of the formation of micelles by LDAO that disperse with increasing temperature, although this was not seen for IpaB or SipB. Another possibility is that because of the dynamic nature of YopB, it may have already formed soluble aggregates or oligomers that disperse as the temperature is raised[17]; however, the importance of this observed decrease in SLS may be minimal because of the relatively large errors seen for the measurements at these lower temperatures.

The biophysical properties of the translocator proteins were collectively analyzed using three-index EPDs (Fig. 1). For IpaB (Fig. 1a), lower temperature regions at pH 7 and 8 (region 1) represent the most properly folded state as observed by the CD signal and fluorescence peak position. Region 2 represents a partially unfolded state of the protein as indicated by the higher Trp peak position observed in low pH environments. Minor aggregation caused by thermal stress is suggested in

DOI 10.1002/jps.24659

region 3. It is noted that the minimal increase in the light scattering intensity, reflecting formation of soluble aggregates that were not detected visually, was still depicted in the EPD as a transition in the structural state. The EPD for SipB (Fig. 1b) showed gradual changes in color and no aggregation regardless of the pH conditions. There were thus only two regions indicated for SipB with region 1 (properly folded state) spanning the entire pH range up to 40°C to 45°C and region 2 seen at higher temperatures. Interestingly, according to the EPD, the most stable region for YopB (region 1; Fig. 1c) appeared to be at around pH 5 up to approximately 60°C. This is probably because of the high transition temperature seen for the YopB secondary structure at this pH. It should be noted, however, that YopB also showed a tendency to aggregate at this pH based on increased light scattering. Region 2 (pH 3–5, from 60°C up to 85°C) may represent a partially unfolded and/or aggregated state of the protein at higher temperatures, whereas region 3 (pH 6–8) represented continuation of region 1 at elevated temperatures (from 25°C to 85°C). A clustering analysis algorithm[15] differentiated region 3 from region 1 probably as a result of the higher Trp peak position and the slight decrease in light scattering intensity seen between 10°C and 20°C for YopB at pH 6–8. Visible aggregates were formed under region 4 conditions, indicating unfolding of YopB. The color patterns seen for YopB look very different from those of IpaB and SipB, which is probably because of the complexity in the SLS data as described above.

Biophysical Characterization of PA–IpaB, PA–SipB, and PA–YopB

The PA domain used to anchor the translocator proteins to the BLPs was engineered at the N-terminus of the proteins because the addition of PA to the C-terminus led to poor expression and degradation. LDAO continued to be included to maintain the solubility of the proteins after the chaperones were removed. These PA–translocator fusion proteins were characterized to determine any influence of the addition of PA domain on the physical stability of the translocator proteins. Chemical degradation was observed for PA–IpaB and PA–SipB at pH 3 as determined by SDS-PAGE, so this condition was again omitted from the study. PA–YopB formed visible aggregates when dialyzed at pH 3–5, so only pH 6–8 was included in the study for this fusion protein. This finding indicated that at lowered pH, the condition that appeared to give YopB alone its best stability, the protein was destabilized by the addition of the PA domain.

Far-UV CD spectroscopy was used to monitor the secondary structure content of PA–IpaB, PA–SipB, and PA–YopB (Supplemental Figs. S4A, S5A, and S6A). Once again, double minima at 208 and 222 nm were observed suggesting that there was conservation of the α-helical secondary structure within these translocator fusion proteins. To monitor retention of the α-helical structure as a function of temperature, the molar ellipticity at 222 nm was monitored (Supplemental Figs. S4B, S5B, and S6B). For PA–IpaB, the molar ellipticity signal gradually decreased with increasing thermal stress regardless of pH until it reached approximately 50°C, suggesting gradual and partial loss of secondary structure. At pH 6–8, there was a minor transition at about 50 °C followed by a major transition at approximately 60°C that indicated a substantial structural alteration. Meanwhile, the secondary structure continued to be gradually lost at pH 4 and 5 as the temperature was increased. No such apparent conformational change for IpaB alone was observed at higher temperatures (Supplemental Fig. S1B). PA–SipB showed patterns similar to PA–IpaB but at different pH conditions in that the protein at pH 4 and 8 resisted the rapid structural changes caused by thermal stress, whereas the unfolding transitions were observed from pH 5 to 7 between 45°C and 50°C (Supplemental Fig. S5B). In contrast to PA–IpaB and PA–SipB, the secondary structure of PA–YopB was found to be very sensitive to changes in pH and temperature of the solution. The secondary structure of PA–YopB started unfolding at approximately 28°C and underwent a second subtle transition at approximately 60°C (seen as a leveling off of the signal change) regardless of pH. For all three proteins, addition of the relatively small PA domain had at least some effect on the secondary structure.

The tertiary structural stability of PA–translocator proteins, as determined by fluorescence peak position, appeared to be significantly influenced by the addition of the PA tag in comparison to each translocator protein alone (Supplemental Figs. S4C, S5C, and S6C). A somewhat similar pattern was observed for all three proteins that started with a gradual red shift followed by a blue shift prior to unfolding. As the temperature initially started to increase, the tertiary structure appeared to be perturbed for each fusion protein as indicated by a red shift in the Trp peak position. This red shift was followed by a blue shift as the temperature was raised, probably as a result of the burying of Trp residues as a result of aggregation. The aggregation corresponding to the blue shift was confirmed by the SLS data (Supplemental Figs. S4D, S5D, and S6D). When considered separately, PA–IpaB at all pH values started to lose tertiary structure and aggregate between 40°C and 50°C. The extent of the blue shift was observed to lessen as the pH of the environment was lowered. PA–SipB exhibited a similar pattern, although the onset of aggregation started at approximately 30°C. Interestingly, PA–IpaB and PA–SipB underwent significant aggregation under neutral rather than acidic pH conditions. PA–YopB appeared to be the least stable as it lost tertiary structure and aggregated starting near 20°C at each pH.

The EPDs of PA–IpaB and PA–SipB showed similar patterns (Figs. 2a and 2b). Region 1 represented the most native-like state at all pH values below about 40°C–50°C. Partial unfolding indicated by the fading of the red color was represented in region 2 for PA–IpaB and the related regions 2 and 3 for PA–SipB. Meanwhile, region 3 (PA–IpaB) and region 4 (PA–SipB) near neutral pH and over 50°C clearly showed some unfolding of the proteins along with the presence of aggregation. Three regions were defined for PA–YopB, but the overall stability at the pH values tested (near neutral pH) seemed to be increased by the addition of the PA domain. Region 1 (at pH 6–8, up to ~30°C) represented the most stable form, whereas region 2 (pH 6–8, from 30°C up to 65°C) indicated a loss of protein structure and the formation of aggregates. Complete aggregation and settling down of visible aggregates occurred in region 3. PA–YopB is clearly much less stable than the other two as observed by the lower onset of aggregation temperature (~30°C), which is easily seen in the EPD (Fig. 2c) as blue-colored regions 2 and 3. The overall structural stability of the translocator proteins was strongly influenced by the addition of the PA domain, even in the presence of LDAO, which was shown to maintain conformational stability of the translocator proteins alone. Among the three proteins, YopB was most adversely influenced by the

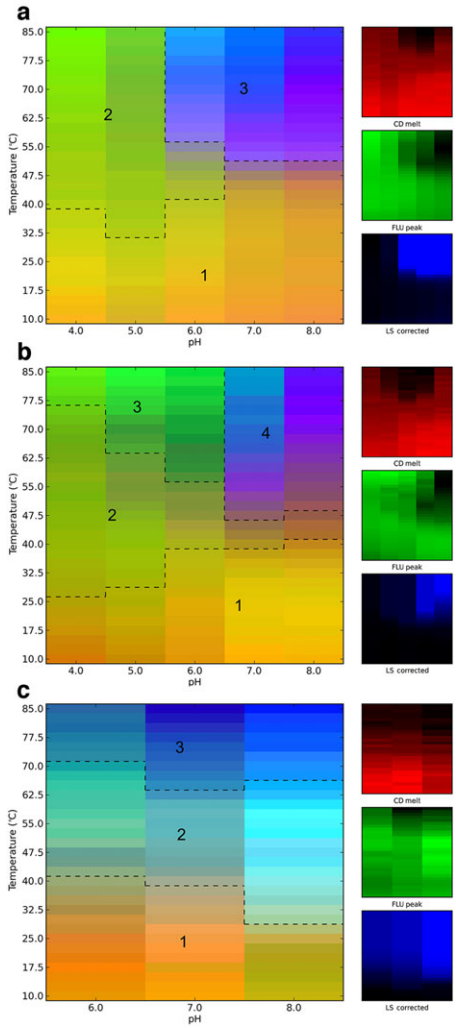

Figure 2. Three-index EPDs with LDAO present for PA–IpaB (a), PA–SipB (b), and PA–YopB (c), representing the conformational stability of the PA–translocator proteins as a function of pH and temperature. The red, green, and blue panels at the right define individual component indices for secondary structure (CD), tertiary structure (fluorescence peak position), and aggregation behavior (LS), respectively.

presence of the PA domain at low pH, although at neutral pH it appeared to be somewhat more thermostable than the YopB alone.

Determining the Effect of Genetic Fusion on PA and Translocator Protein Stability Using DSC

Although the spectroscopic methods used for generating EPDs for the PA–translocator protein complexes indicated differences in behavior for each of the translocator proteins following fusion with the PA anchor, these methods do not distinguish between the contributions made by each part of the fusion to the final spectroscopic signals. This is especially true for CD signals where both proteins have predominantly α-helical signals (see Supplemental Figs. S1a, S2a, S3a, and S7a) and therefore it would be difficult to determine how each influences the stability of the resulting fusion. To overcome this potential problem, DSC was used at pH 7 to compare the transitions occurring within PA alone, the translocator proteins alone, and the

Table 1. Structural Transitions Determined Using Differential Scanning Calorimetry

	Observed Transition Temperature (°C)[a]		
Protein	Transition 1	Transition 2	Transition 3
PA alone[b]	36.54 ± 0.52	40.37 ± 0.27	85.64 ± 0.41
IpaB alone	48.03 ± 0.06	Not observed	Not observed
PA–IpaB	49.11 ± 0.24	51.84 ± 0.18	88.23 ± 0.04
SipB alone	39.61 ± 0.19	Not observed	Not observed
PA–SipB	41.09 ± 0.10	44.00 ± 0.20	85.43 ± 0.21
YopB alone	34.00 ± 1.00	40.00 ± 0.00	Not observed
PA–YopB	43.91 ± 0.10	47.00 ± 0.24	84.29 ± 0.40

[a]Data shown are an average of a minimum of two separate scans (see Supplemental Information) ±SD. All measurements were obtained at pH 7.0 in 20 mM citrate phosphate buffer with an ionic strength of 0.15 using NaCl as was performed for the spectroscopic analyses.
[b]The peptidoglycan anchor (PA) domain was prepared in the absence of a fused translocator partner to determine its behavior alone in solution.

PA–translocator fusions. When DSC was performed on PA alone, three endotherms were observed with two major peaks near 40°C and a very minor one near 85°C (Table 1; Supplemental Fig. S8). The major peaks were at lower temperatures than the major transitions seen by CD analysis, but did correspond to minor transitions seen by CD and fluorescence spectroscopy (see Supplemental Figs. S7 and S8). Because the major transitions seen by DSC did not precisely correlate with the major transition seen in secondary structure by CD spectroscopy, it is possible that the DSC signals represent transition to a less tightly packed structure or a molten globule-like state prior to loss of secondary structure.

When DSC was used to analyze each translocator protein, a single peak was observed for IpaB and SipB with one major and a minor peak observed for YopB (Table 1; Supplemental Figs. S9–S11). Interestingly, when the PA–translocator protein fusions were analyzed by DSC, three endotherms were observed rather than the expected four (or five) where three are contributed by the PA and the others by the translocator protein. It would be unexpected for the translocator signal to be completely lost by this method, but when the two major peaks of these fusions were closely examined, it was found that they occurred at temperatures higher than PA alone and for the translocator proteins alone (Table 1). These data indicate that the fusions actually appear to be more stable overall than either of the individual components. This mutual stabilization was not anticipated; however, it was significant and was relatively consistent for each of the three translocator proteins. On the contrary, stabilization of the PA portion of the PA–IpaB fusion was substantial with the two peaks going from 37°C and 40°C to 49°C and 52°C, respectively (Table 1; Supplemental Figs. S8 and S9). Thus, it appears that PA and the translocator proteins have a mutually stabilizing effect when analyzed by DSC.

Biophysical Characterization of IpaB–BLP, SipB–BLP, and YopB-BLP

For all of the proteins associated with BLPs, the BLP particles tended to dominate the spectroscopic signals. Because of problems with either protein degradation or early aggregation of the PA–translocator proteins as mentioned previously, IpaB–BLP and SipB–BLP complexes were only characterized from pH 4

DOI 10.1002/jps.24659

to 8, whereas YopB–BLP was again studied from pH 6 to 8. The far-UV CD spectra at 10°C for all the tip-BLPs also showed a single dominant minimum at approximately 225 nm (Supplemental Figs. S12A, S13A, and S14A) with much less signal seen at pH 4 and 5 for IpaB–BLPs, and pH 4–6 for SipB–BLPs. As a general trend for IpaB–BLPs and SipB–BLPs, the CD signals at pH 4 and 5 decreased immediately after thermal stress was applied. Higher transition temperatures were recorded for both proteins in neutral pH environments; however, it was lower than that seen for the protein–PA fusions alone (Supplemental Figs. S12B and S13B). Transitions were clearly evident as observed by sharp decrease in signals for the IpaB–BLP and SipB–BLP complexes. Furthermore, the secondary structure appeared to be completely lost after the unfolding process was complete. The YopB–BLPs, however, behaved very differently with the overall secondary structure retained throughout the process without significant transitions (Supplemental Fig. S14B). Moreover, the secondary structure of YopB–BLPs was better maintained at pH 8.

The integrity of the protein–BLP complexes was examined with regard to the tertiary structure of the proteins using intrinsic fluorescence peak position. (Supplemental Figs. S12C, S13C, and S14C). For IpaB–BLPs and SipB–BLPs, the peak of the Trp fluorescence spectra displayed a gradual redshift as the thermal stress was increased. Essentially, in agreement with the CD data, both complexes displayed improved physical stability around neutral pH when compared with lower pH environments. This instability at lower pH was more evident for SipB–BLPs than for IpaB–BLPs. Nonetheless, the tertiary structure of the complex was observed to be stable up to approximately 40°C at pH 7 and 8. Meanwhile, the tertiary structure of YopB–BLPs seemed to be maintained relatively well as no sharp transition was evident in the peak position data for YopB–BLPs with increasing thermal stress.

Aggregation of the protein–BLPs complex was again monitored using SLS spectroscopy. The IpaB–BLPs and SipB–BLPs (Supplemental Figs. S12D and S13D) demonstrated a rapid drop in signal that was attributed to the protein aggregating, thus causing the BLPs to precipitate and fall out of solution. Such a precipitation event leading to loss of BLPs from the solution was not observed in a previous study when these same analyses were applied to BLPs alone.[19] Interestingly, a sharp drop in intensity was observed for YopB–BLPs followed by a leveling off to produce a gradual decrease without complete settling of the BLPs unlike the other two protein–BLP complexes (Supplemental Fig. S14D). This unusual behavior might indicate a self-limited structural change occurring at lower temperatures at the beginning and the protein retaining this state as the temperature continues to rise. In general, the integrity of the protein–BLP systems was found to be best maintained under neutral pH conditions.

The three-index EPDs for IpaB–BLP and SipB–BLP exhibited similar patterns with only two defined regions (Figs. 3a and 3b). Region 1 at neutral pH and up to 40°C represented a more native-like state as indicated by the CD, fluorescence peak, and SLS panels on the right. At pH 4 and 5, however, the EPDs detected less to almost no secondary structure as observed by the CD data. Sharp color transitions were observed as stress was applied that led to settling out of the precipitated protein–BLPs complexes. The rest of the EPD was defined as region 2 with blue color indicating an aggregated state. As observed

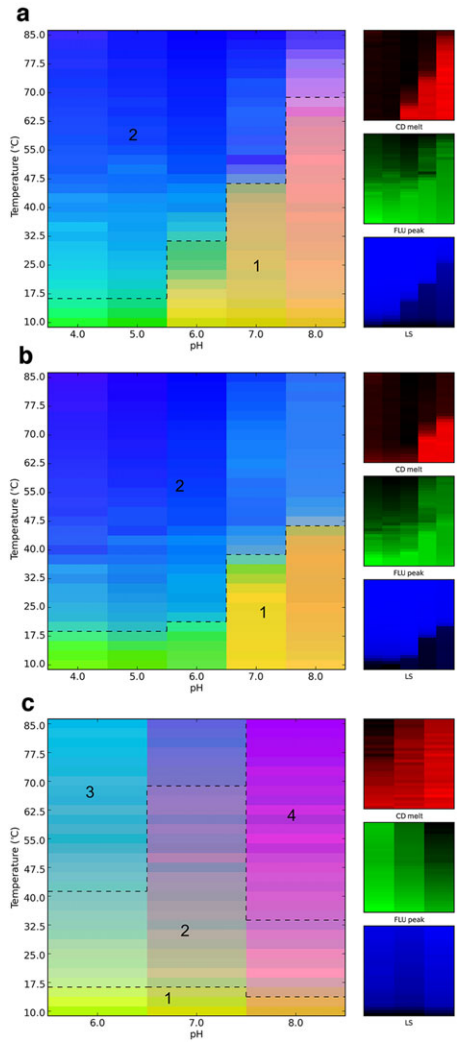

Figure 3. Three-index EPDs with LDAO present for IpaB–BLPs (a), SipB–BLPs, (b) and YopB–BLPs (c), representing the conformational stability of the translocator proteins associated with BLPs as a function of pH and temperature. The red, green, and blue panels at the right define individual component indices for secondary structure (CD), tertiary structure (fluorescence peak position), and aggregation behavior (SLS), respectively.

earlier, the YopB–BLPs behaved differently than IpaB–BLPs and SipB–BLPs. Following an initial decrease in light scattering signal, the sample started to quickly enter an aggregated state. Meanwhile, the color changes in secondary and tertiary panels arise from the gradual, though detectable, transitions in the CD and peak position signals. The rather small region 1 thus represents the most stable state, whereas regions 2, 3, and 4 represent varying degrees of structural perturbation that arise from the combined effects of the different secondary and tertiary structure states seen under different environmental stresses.

One thing to note concerning the EPDs for BLP-containing complexes is the complexity of these systems and the dominance of the particles in the resulting spectroscopic signals. Unfortunately, the complexity is rather overwhelming even for other biophysical methods (e.g., calorimetry). Nevertheless, translocator proteins on the surface of BLPs can dramatically

alter the solution behavior of these particles as shown by their precipitation under conditions expected to push the proteins into an aggregative state (Supplemental Figs. S15D, S16D, and S17D). No such precipitation with subsequent settling out of solution occurs for BLPs alone as was previously reported.[19] Thus, SLS is probably the best indicator of BLP complex stability, whereas the other methods used here provide a better picture of the behavior of the fusion proteins prior to being bound to the BLPs. With regard to the stability of the translocators as they are fused to PA and then loaded onto BLPs, supplemental figures are provided for each translocator alone, as it is fused with PA and then as the fusion is bound to the BLPs at pH 7 to allow a direct comparison (Supplemental Figs. S15–S17). The pH 7 condition was selected for these figures because neutral or near-neutral conditions appeared to provide the most stable environment across the board for these proteins. These figures are derived from the earlier supplemental figures, but are shown here because they provide a direct comparison of how fusion with PA and anchoring to the BLP surface affects each of the proteins. The individual spectroscopy data do not seem to show that fusion with PA has an obvious stabilizing effect on translocator proteins; however, this does appear to be the case at neutral pH according the EPDs and this is consistent with the DSC measurements for each translocator and PA–translocator fusion.

DISCUSSION

Bacterium-like particles represent a potentially valuable presentation platform for protein subunit vaccines as they present antigen in a polymeric form with a peptidoglycan shell that serves as an intrinsic adjuvant that stimulates innate immune pathways.[6] In this study, we used a variety of biophysical techniques to characterize the solution properties of T3SS translocator proteins from *S. flexneri*, *S. typhimurium*, and *Y. enterocolitica* incorporated into a novel BLP vaccine platform. These translocator proteins are potential protective antigens against infections caused by their corresponding bacterial pathogens.[20] Thus, we conducted this stability study to determine whether future formulation studies (required to optimize vaccine delivery and efficacy) are possible. Biophysical techniques such as CD, intrinsic fluorescence, and SLS spectroscopies were used to assess the structural stability of these proteins alone, as fusion proteins with a PA domain, and the latter after association with BLP particles. The acquired data sets were then summarized in a three-index EPD to allow comprehensive visualization of the physical states of the proteins in response to varying pH and temperature conditions.

These translocator proteins also play essential roles in the virulence of their respective pathogens by creating a pore in target cell membranes and, in some cases, acting directly as effector proteins that alter host cell activities.[21] In their dual roles, they are attractive as vaccine targets, although their hydrophobic nature necessitates inclusion of a detergent to maintain solubility. The mild detergent LDAO was used here for preparing all three hydrophobic translocator proteins based on its success with IpaB.[22] Moreover, LDAO has been shown to inhibit dramatic structural alterations and aggregation in previous studies on of a DB fusion protein vaccine candidate.[16] This indeed appears to be the case for IpaB and SipB that retained many of their structural properties in response to thermal stress in the presence of LDAO. When compared, IpaB and SipB were found to behave similarly, whereas YopB displayed different biophysical properties, consistent with the first two belonging to one T3SS family and the latter belonging to another based on sequence similarities and the behavior of their respective T3SS needle tip proteins.[18]

For all the three translocator proteins, the addition of a 25-kDa PA domain at the C-terminus led to destabilization as determined by their degradation during purification (data not shown). Therefore, the PA domain was fused to the N-terminus of each protein. Once again, PA–IpaB and PA–SipB behaved similarly relative to each other. Both displayed slightly different structural behavior, however, relative to the proteins lacking the PA domain, according to the EPDs. PA–YopB displayed the most dramatic change in behavior relative to the translocator lacking the PA domain. It appears from the EPD that PA–YopB may be stabilized by the addition of the small 25 kDa PA domain when under neutral pH conditions. It was dramatically destabilized, however, under acid pH conditions. Thus, it appears that the presence of an N-terminal PA domain has the greatest effect on YopB, which may be related to the fact that this translocator appears to be less stable in solution than its *Shigella* and *Salmonella* counterparts, even when LDAO is present.

Once each protein was associated with the BLPs, the particles dominated the spectroscopic signals, especially with regard to aggregation. This is probably because of the fact that the particulate nature of the BLPs allowed what would otherwise be soluble aggregates to form large clumps that could quickly settle out of solution. Nevertheless, useful data related to each protein's structural behavior could still be acquired. All of the BLP complexes were compromised at low pH, although the IpaB–BLPs and SipB–BLPs were reasonably thermostable at neutral pH. In contrast, the EPD of the YopB–BLP suggests that this antigen presentation platform is inherently unstable for this protein and is prone to aggregation under all pH conditions tested. Thus, it is possible that the BLP platform may provide a useful means for antigen presentation in vaccines against *Shigella* and *Salmonella* infection, but work remains to stabilize this system for presentation of *Yersinia* translocator proteins. It should be noted, however, that another *Yersinia*-protective antigen is the T3SS needle tip protein (LcrV) and it remained stable[19] and provided mice with protection from lethal challenge by the system pathogen *Yersinia pestis*.[10]

In this study, a diverse set of biophysical data was collected for compilation into three-index EPDs to assess the utility of the BLP platform for presentation of T3SS translocator protein-based vaccines. The results suggest that vaccines to protect against shigellosis and salmonellosis using the BLP presentation platform are certainly possible. Much work, however, remains to stabilize YopB when associated with BLP surfaces. The fact that YopB is less stable in solution containing LDAO than IpaB and SipB probably has a role in its behavior as part of BLP particles. It is possible that different detergents may help stabilize YopB for use in the BLP system and it is likely that this will also be the case for the presentations of other translocator proteins from the *Yersinia* T3SS family (e.g., PopB from *Pseudomonas aeruginosa*). Despite these observations with YopB, the BLP platform does appear to be potentially useful in future vaccine studies involving T3SS translocator proteins.

ACKNOWLEDGMENTS

This work was supported, in part, by grants the NIH (1R01 AI089519) to W.L.P. and NIH (1R01 AI099489) to W.D.P. We thank the members of the Picking laboratory for critical discussions and review of the manuscript. We also thank Jamie C. Greenwood II and Daniel Picking for assistance in protein expression and purification and Ozan Kumru for assistance with biophysical analyses.

REFERENCES

1. Kotloff KL, Nataro JP, Blackwelder WC, Nasrin D, Farag TH, Panchalingam S, Wu Y, Sow SO, Sur D, Breiman RF, Faruque AS, Zaidi AK, Saha D, Alonso PL, Tamboura B, Sanogo D, Onwuchekwa U, Manna B, Ramamurthy T, Kanungo S, Ochieng JB, Omore R, Oundo JO, Hossain A, Das SK, Ahmed S, Qureshi S, Quadri F, Adegbola RA, Antonio M, Hossain MJ, Akinsola A, Mandomando I, Nhampossa T, Acacio S, Biswas K, O'Reilly CE, Mintz ED, Berkeley LY, Muhsen K, Sommerfelt H, Robins-Browne RM, Levine MM. 2013. Burden and aetiology of diarrhoeal disease in infants and young children in developing countries (the Global Enteric Multicenter Study, GEMS): A prospective, case-control study. Lancet 382(9888):209–222.

2. Kolling G, Wu M, Guerrant RL. 2012. Enteric pathogens through life stages. Front Cell Infect Microbiol 2:114.

3. Galan JE, Wolf-Watz H. 2006. Protein delivery into eukaryotic cells by type III secretion machines. Nature 444(7119):567–573.

4. Schroeder GN, Hilbi H. 2008. Molecular pathogenesis of *Shigella* spp.: Controlling host cell signaling, invasion, and death by type III secretion. Clin Microbiol Rev 21(1):134–156.

5. Audouy SA, van Selm S, van Roosmalen ML, Post E, Kanninga R, Neef J, Estevao S, Nieuwenhuis EE, Adrian PV, Leenhouts K, Hermans PW. 2007. Development of lactococcal GEM-based pneumococcal vaccines. Vaccine 25(13):2497–2506.

6. Leenhouts K. 2013. Mimopath-based vaccine delivery. In Novel immune potentiators and delivery technologies for next generation vaccines; Singh M, Ed. New York: Springer, pp 245–265.

7. Mattia A, Merker R. 2008. Regulation of probiotic substances as ingredients in foods: Premarket approval or "generally recognized as safe" notification. Clin Infect Dis 46 Suppl 2:S115–S118; discussion S144–S151.

8. Mshvildadze M, Neu J, Mai V. 2008. Intestinal microbiota development in the premature neonate: Establishment of a lasting commensal relationship? Nutr Rev 66(11):658–663.

9. Keijzer C MT, Voorn P, de Haan A, Haijema BJ, Leenhouts K, van Roosmalen ML, van Eden W, Broere F. 2014. Inactivated influenza vaccine adjuvanted with bacterium-like particles induce systemic and mucosal influenza A virus specific T-cell and B-cell responses after nasal administration in a TLR2 dependent fashion. Vaccine 32(24):2904–2910.

10. Ramirez K, Ditamo Y, Rodriguez L, Picking WL, van Roosmalen ML, Leenhouts K, Pasetti MF. 2010. Neonatal mucosal immunization with a non-living, non-genetically modified Lactococcus lactis vaccine carrier induces systemic and local Th1-type immunity and protects against lethal bacterial infection. Mucosal Immunol 3(2):159–171.

11. Bosma T, Kanninga R, Neef J, Audouy SA, van Roosmalen ML, Steen A, Buist G, Kok J, Kuipers OP, Robillard G, Leenhouts K. 2006. Novel surface display system for proteins on non-genetically modified gram-positive bacteria. Appl Environ Microbiol 72(1):880–889.

12. de Haan A, Haijema BJ, Voorn P, Meijerhof T, van Roosmalen ML, Leenhouts K. 2012. Bacterium-like particles supplemented with inactivated influenza antigen induce cross-protective influenza-specific antibody responses through intranasal administration. Vaccine 30(32):4884–4891.

13. Nganou-Makamdop K, van Roosmalen ML, Audouy SA, van Gemert GJ, Leenhouts K, Hermsen CC, Sauerwein RW. 2012. Bacterium-like particles as multi-epitope delivery platform for Plasmodium berghei circumsporozoite protein induce complete protection against malaria in mice. Malaria J 11:50.

14. Rigter A, Widjaja I, Versantvoort H, Coenjaerts FE, van Roosmalen M, Leenhouts K, Rottier PJ, Haijema BJ, de Haan CA. 2013. A protective and safe intranasal RSV vaccine based on a recombinant prefusion-like form of the F protein bound to bacterium-like particles. PLoS One 8(8):e71072.

15. Kim JH, Iyer V, Joshi SB, Volkin DB, Middaugh CR. 2012. Improved data visualization techniques for analyzing macromolecule structural changes. Protein Sci 21(10):1540–1553.

16. Chen X, Choudhari SP, Martinez-Becerra FJ, Kim JH, Dickenson NE, Toth RT, Joshi SB, Greenwood 2nd JC, Clements JD, Picking WD, Middaugh CR, Picking WL. 2015. Impact of detergent on biophysical properties and immune response of the ipadb fusion protein, a candidate subunit vaccine against *shigella* species. Infect Immun 83(1):292–299.

17. Mukherjee A, Lutkenhaus J. 1999. Analysis of FtsZ assembly by light scattering and determination of the role of divalent metal cations. J Bacteriol 181(3):823–832.

18. Choudhari SP, Chen X, Kim JH, van Roosmalen ML, Greenwood 2nd JC, Joshi SB, Picking WD, Leenhouts K, Middaugh CR, Picking WL. 2014. Biophysical characterization of the type iii secretion tip proteins and the tip proteins attached to bacterium-like particles. J Pharm Sci 104(2):424–432.

19. Martinez-Becerra FJ, Scobey M, Harrison K, Choudhari SP, Quick AM, Joshi SB, Middaugh CR, Picking WL. 2013. Parenteral immunization with IpaB/IpaD protects mice against lethal pulmonary infection by Shigella. Vaccine 31(24):2667–2672.

20. Ogawa M, Handa Y, Ashida H, Suzuki M, Sasakawa C. 2008. The versatility of *Shigella* effectors. Nat Rev 6(1):11–16.

21. Dickenson NE, Choudhari SP, Adam PR, Kramer RM, Joshi SB, Middaugh CR, Picking WL, Picking WD. 2013. Oligomeric states of the Shigella translocator protein IpaB provide structural insights into formation of the type III secretion translocon. Protein Sci 22(5):614–627.

22. Markham AP, Birket SE, Picking WD, Picking WL, Middaugh CR. 2008. pH sensitivity of type III secretion system tip proteins. Proteins 71(4):1830–1842.